

Lattice dynamics of single-walled achiral BC₃ nanotubes

Z. X. Guo,¹ Y. Xiao,¹ J. W. Ding,^{1,2,*} and X. H. Yan³

¹*Department of Physics, Xiangtan University, Xiangtan 411105, Hunan, China*

²*National Laboratory of Solid State Microstructures, Nanjing University, Nanjing 210093, China*

³*College of Science, Nanjing University of Aeronautics and Astronautics, Nanjing 210016, China*

(Received 30 July 2005; revised manuscript received 18 October 2005; published 9 January 2006)

The phonon dispersion relation and specific heat of single-walled BC₃ nanotubes have been investigated using a force constant model. The obtained phonon dispersion relation of BC₃ sheet reproduces well the experimental data. The tube-diameter dependent frequencies of both the radial breathing mode and the lowest phonon mode E_{2g} can be well fitted by a power law $\omega=C/R^\alpha$ with tube radius R , where the scaling exponent $\alpha=1$ and the proportional constant $C=939.6\text{ cm}^{-1}\text{ \AA}$ in the former and $\alpha=1.1$ and $C=321.5\text{ cm}^{-1}\text{ \AA}^{1.1}$ in the latter, at variance with carbon nanotubes and BN nanotubes. The specific heat of BC₃ nanotubes are also calculated, less than that of the BC₃ sheet, in which several crossings are observed at low temperature due to the first optical phonon mode excited at different temperature. By virtue of the simple zone-folding model, in addition, a universal formula is derived to describe the tube diameter dependence of specific heat for various types of nanotube systems. The results provide an alternative way to characterize the BC₃ nanotubes and suggest the underlying quantized phonon structures in one-dimensional nanotube systems.

DOI: [10.1103/PhysRevB.73.045405](https://doi.org/10.1103/PhysRevB.73.045405)

PACS number(s): 61.46.-w, 63.22.+m, 65.40.Ba

I. INTRODUCTION

BC₃ nanotubes (BCNTs) have been studied both theoretically and experimentally due to its unique physical properties.¹ For instance, electronic structure calculations indicated that the band gaps of BCNTs are insensitive to the diameter and chirality,^{2,3} different from that of carbon nanotubes (CNTs), while their mechanical properties can be comparable to that of CNTs.⁴ Owing to the different geometrical structures and compositions, especially, BCNTs are expected to exhibit some outstanding thermal properties such as specific heat and thermal transport. From a practical point of view, good thermal managements of BCNTs have potential applications of future nanotube-based thermoelectrical devices, which can greatly improve performances of the nano-sized devices due to heat dissipations.

A very useful tool for the characterization of BCNTs is Raman spectroscopy, which is widely used in the estimation of diameter distribution of CNTs.⁵ In order to assign the Raman peaks of BCNTs, one needs to calculate the phonon modes of BCNTs. This means that lattice dynamics of BCNTs may be of particular importance in the characterization and thermal managements in the BCNT-based molecular devices. As quasi-one dimensional (1D) nano functional materials, additionally, the lattice dynamics of CNTs and BN nanotubes have been investigated in details, showing up some singular thermal properties.^{6,7} The study of lattice dynamics of BCNTs would be very helpful to explore quantum size effects and universal laws of thermal properties of quasi-1D nanotube systems.

On the other hand, the structure of BC₃ hexagonal sheet may be very similar to that of Mg₂BC₃ with high superconducting transition temperature.⁸ From a microscopic point of view, the electron-phonon coupling is one of the dominating mechanisms for superconducting states. Therefore, the phonon calculations of BCNTs can contribute to understanding of the underlying superconducting mechanism of BC₃-based

compounds. In this paper, we perform the lattice dynamics calculations of the BC₃ sheet and BCNTs within a force constant model. The results show that the phonon structures of BCNTs are very different from that of CNTs. Combined with its uniform energy gap, the BCNT may be a suitable candidate in future thermoelectrical nanodevices.

II. FORCE CONSTANT MODEL

Due to the nature of two-dimensional (2D) sheet, one can build a force constant model to study the phonon dispersion relation (PDR) of BCNT.⁹⁻¹² Based on such a model, the experimentally observed Raman modes of CNT samples had been reproduced well.¹³⁻¹⁷ Here we firstly calculate the PDR of BC₃ sheet to fit the experimental phonon spectra of BC₃ sheet. In this model, it is crucial to determine force constants between two atoms. Similar to the graphite sheet,^{9,10} only 3×3 force constant matrices within the fourth nearest neighboring distance are required to generate the dynamical matrix $D(k)$ of the BC₃ sheet. In order to fit the experimental phonon spectra of the BC₃ sheet, the force constant parameters are presented in Table I, in which $\phi_r^{n(A-B)}$, $\phi_{ii}^{n(A-B)}$, and $\phi_{to}^{n(A-B)}$ represent force constants between A atom and B atom (B atom is the n th nearest neighbor of A atom) in the radial, in-plane tangential and out-of-plane direction. With these parameters, we calculate in Fig. 1 the PDR of the BC₃ sheet. From Fig. 1, one longitudinal acoustic (LA) branch and one transverse acoustic (TA) branch have been obtained with linear dispersion, while another TA branch with quadratic wave-vector dependence.¹⁸⁻²⁰ The quadratic behavior can be explained by the fact that this mode is a 2D mode in BC₃ sheet with n -fold ($n \geq 3$) rotational symmetry. Moreover, the majority of experimental phonon branches²¹ are reproduced by present model. Good agreement between our theoretical results and experiments shows that the parameters presented in Table I are reasonable.

TABLE I. Force constants of the BC₃ sheet in units of 10⁴ dyn cm⁻¹.

Radial	Tangential	
$\phi_r^{1(C-C)}=32.0$	$\phi_{ii}^{1(C-C)}=23.0$	$\phi_{to}^{1(C-C)}=8.5$
$\phi_r^{1(B-C)}=28.0$	$\phi_{ii}^{1(B-C)}=18.0$	$\phi_{to}^{1(B-C)}=5.8$
$\phi_r^{2(C-C)}=8.00$	$\phi_{ii}^{2(C-C)}=-3.00$	$\phi_{to}^{2(C-C)}=-0.3$
$\phi_r^{2(B-C)}=5.00$	$\phi_{ii}^{2(B-C)}=-3.5$	$\phi_{to}^{2(B-C)}=-0.40$
$\phi_r^{2(C-C)}=7.0$	$\phi_{ii}^{2(C-C)}=-2.80$	$\phi_{to}^{2(C-C)}=-0.25$
$\phi_r^{3(C-C)}=2.50$	$\phi_{ii}^{3(C-C)}=-5.0$	$\phi_{to}^{3(C-C)}=0.3$
$\phi_r^{3(B-B)}=1.0$	$\phi_{ii}^{3(B-B)}=-3.50$	$\phi_{to}^{3(B-B)}=0.7$
$\phi_r^{3(C-C)}=2.0$	$\phi_{ii}^{3(C-C)}=-4.5$	$\phi_{to}^{3(C-C)}=0.5$
$\phi_r^{4(B-C)}=-1.8$	$\phi_{ii}^{4(B-C)}=1.0$	$\phi_{to}^{4(B-C)}=-0.22$
$\phi_r^{4(C-C)}=-1.9$	$\phi_{ii}^{4(C-C)}=2.0$	$\phi_{to}^{4(C-C)}=-0.55$

III. RESULTS AND DISCUSSION

A. Phonon dispersion relations

In an BCNT, the force constant matrix can be obtained by rotating the bond from the 2D plane to 3D cylindrical coordinate system. The PDR of BCNTs can be further calculated. As an example, we show in Fig. 2 the PDRs of zigzag (4,0) and armchair (4,4) BCNTs. Compared with 2D BC₃ sheet, there are four acoustic modes at around Γ point from PDR of BCNTs: Two degenerate TAs, one LA, and one twisting (TWA). The TA and LA modes have linear dispersions at low energy, while there is a problem of nonzero frequency in the

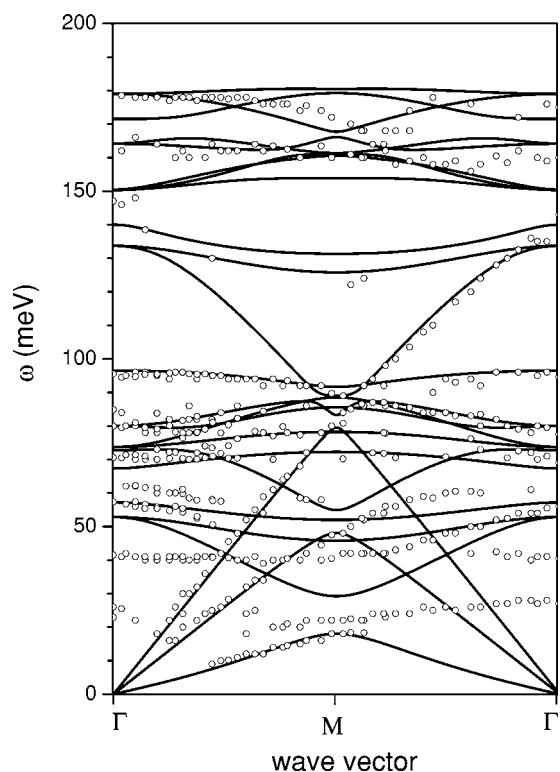


FIG. 1. Calculated phonon dispersion relation of the BC₃ sheet (solid lines) together with the experimental points (open circles).

TWA mode, just as in the CNT case.^{9,12} To avoid the unphysical result, an improved method was proposed by Saito *et al.*⁹ and Dobardzic *et al.*¹² In present calculations of BCNTs, the force constants have been rescaled using the Saito's method. The calculated frequency of TWA mode at Γ point is close to zero, similar with that in the CNT case.⁹ It may be expected that the exact zero frequency of TWA mode can be obtained provided that a projecting method is applied, as in Ref. 12. As a result, the dispersion of TWA mode appears to be linear at around Γ point. From Fig. 2, also, the highest frequency in PDR is obtained to be about 1450 cm⁻¹, lower than 1600 cm⁻¹ of CNT,⁹⁻¹² which may be attributed to the weak bonding in BCNTs. This indicates that BCNTs are less stiff than CNTs, consistent with the tight binding calculations.⁴

From Fig. 2, interestingly, it is seen that there are 120 distinct phonon branches, of which 48 branches are nondegenerate and 72 branches are doubly degenerate. The number N_{BCNT} of distinct phonon branches of both armchair (n, n) and zigzag ($n, 0$) BCNTs can be expressed by

$$N_{BCNT} = 48 + 24(n - 1). \quad (1)$$

This relation has an analogy to that of achiral CNTs^{7,22} with $N = 12 + 6(n - 1)$. Then we have

$$N_{BCNT} = 4N_{CNT}. \quad (2)$$

From space group theory, N_{CNT} can be obtained from the analysis of irreducible representation of CNTs.^{7,22} Therefore, Eqs. (1) and (2) provide an alternative way to check the classifications of phonon modes of BCNT.²³ Such a classification of BCNTs is not done so far, and thus the relation in Eq. (2) is a significant result.

In Figs. 2(b) and 2(d), we show the corresponding density of states (DOS), $g(\omega)$, of the (4,0) and (4,4) BCNTs. One notices that in the low energy region, the DOS curves are very flat for the two kinds of BCNTs. This is the consequence of one dimensionality of BCNTs. In d -dimensional system, usually, it follows $g(\omega) \propto \omega^{d\alpha-1}$ for an acoustic phonon branch of $E(q) \propto q^\alpha$. For the 2D BC₃ sheet, for example, the dispersion $E(q) \propto q^2$ of the out-of-plane phonon leads to $g(\omega) = \text{constant}$. In an BCNT, $g(\omega)$ is dominated by the linear acoustic modes at low energy, and thus $g(\omega)$ is also a constant, similar to that of the 2D BC₃ sheet. Another important feature in DOS is the first peak, originated from the first optical phonon mode, which depends on the tube diameter of BCNTs. When rolling an BC₃ sheet into an BCNT, the circumferential quantization of wave vector results in the splitting of the phonon modes into multiply subbands, showing up some sharp peaks in the DOS. The first peak is associated to the first optical phonon mode (the first subband), which is shifted to higher frequency with the decrease of tube diameter. This mode has an important effect on the specific heat of BCNTs, discussed in detail below. Especially, the first optical phonon mode ω_{op} is excited at temperature $T_{op} = \hbar \omega_{op} / k_B$ with k_B and \hbar the Boltzmann constant and the Planck constant, so that the quantization of thermal conductance may be easily observed below T_{op} . Small diameter tube with the smooth contacts would be preferred to get high T_{op}

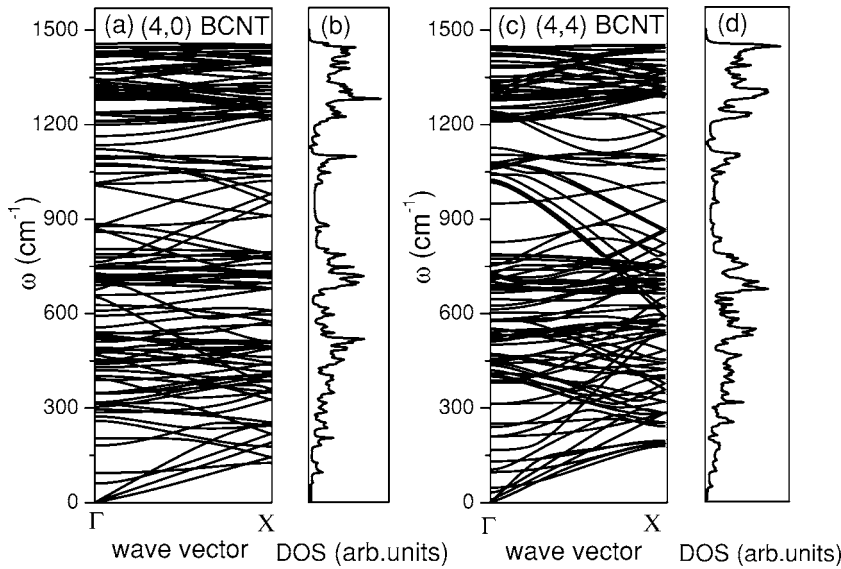


FIG. 2. (a) PDR and (b) DOS of zigzag (4,0) BCNT; (c) PDR and (d) DOS of armchair (4,4) BCNT.

due to the high frequency ω_{op} . Therefore, the first optical phonon mode plays an essential role in quantization of thermal conductance,²⁴ especially for very narrow BCNTs.

Of all phonon modes, an important mode is the radial breathing mode (RBM), in which all atoms of a nanotube move in the radial direction with the in-phase displacements, as shown in Fig. 3(a) inset. We calculate in Fig. 3(a) the frequency of RBM of BCNT as a function of tube radius R . Obviously, the frequency of RBM increases with R decreasing, which can be fitted by

$$\omega_{RBM} = A/R, \quad (3)$$

with $A=939.6 \text{ cm}^{-1} \text{ \AA}$ the proportional constant. The scaling relation, Eq. (3), is similar to that of CNTs, however, the constant A is lower than $1170.0 \text{ cm}^{-1} \text{ \AA}$ of CNTs.²⁵ The RBM can be used in the characterization of BCNT samples, as in the case of CNTs.¹³⁻¹⁷ To further clarify the tube diameter dependence of various modes, also, Fig. 3(b) shows the lowest phonon mode E_{2g} as a function of R . This mode has

the xy and x^2-y^2 symmetries,⁹ as shown by Fig. 3(b) inset. The frequency of the E_{2g} mode increases with R decreasing, similar to that of RBM. The fitting formula is obtained by

$$\omega_{E_{2g}} = B/R^{1.1}, \quad (4)$$

with $B=321.5 \text{ cm}^{-1} \text{ \AA}^{1.1}$. The decay exponent in Eq. (4) is larger than that in Eq. (3), showing the distinct dependence of the various modes on the tube diameter. For small diameter BCNTs, in addition, there appears a deviation from the fitting formula. This can be attributed to the strong curvature effect in small diameter nanotubes, which has been demonstrated in detail based on the curvature energy.²⁶ To satisfy the requirements in nanotube-based device applications, the characterization of BCNTs is very necessary. The scalings of Eqs. (3) and (4) would be helpful in the future to characterize BCNTs for fast selection in nanotube samples.

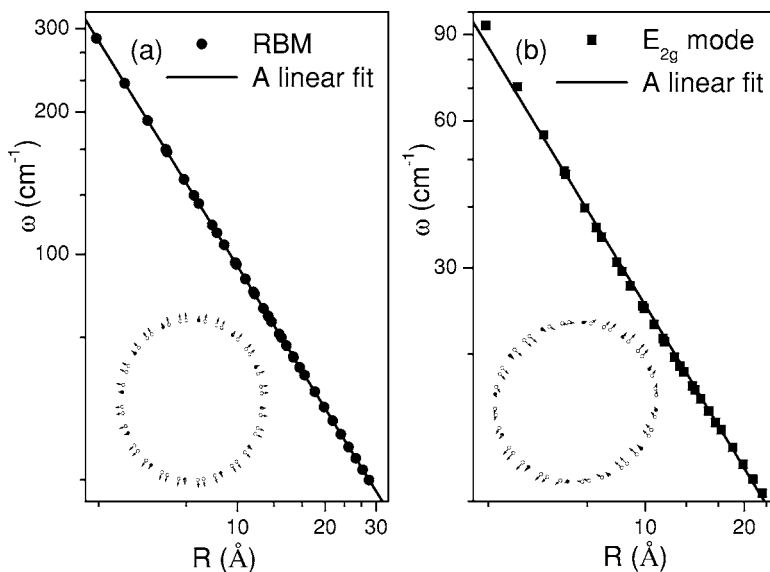
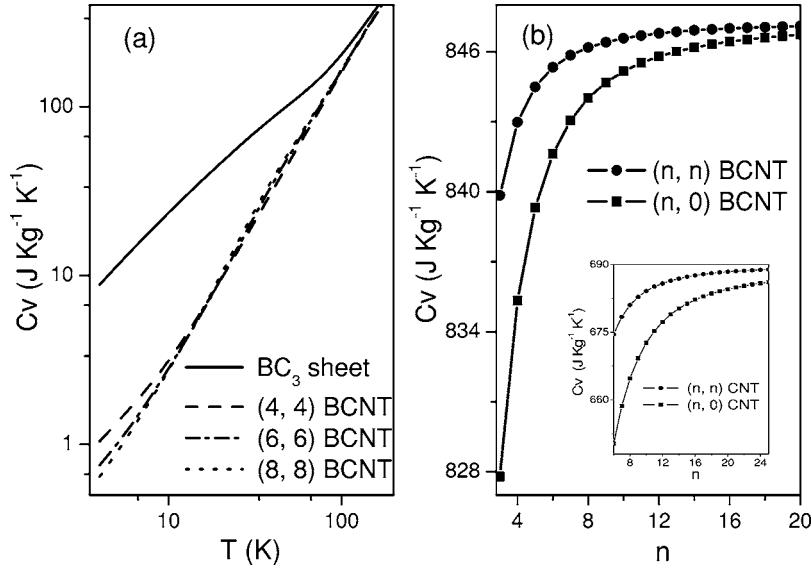


FIG. 3. Frequencies of (a) RBM and (b) E_{2g} of achiral BCNTs as a function of radius. The solid lines are a linear fit to the data for BCNTs. In the insets, the open and solid circles represent the vibrational patterns of carbon and boron atoms, respectively.



B. Specific heat

To explore the thermal properties in BCNT-based nanodevices, we can further calculate the specific heat $C_V(T)$ of both the BC_3 sheet and BCNTs in terms of the obtained DOS. Here $C_V(T)$ is defined by

$$C_V(T) = \frac{\hbar^2}{k_B T^2} \int_0^{\omega_{\max}} \frac{\omega^2 \exp(\hbar\omega/k_B T)}{(\exp(\hbar\omega/k_B T) - 1)^2} g(\omega) d\omega. \quad (5)$$

In Fig. 4(a), we plot the specific heat of the BC_3 sheet and the (n,n) BCNTs ($n=4,6,8$). From Fig. 4(a), C_V of both the BC_3 sheet and BCNTs increase with temperature T , finally approaching the classical limit (not fully shown), independent of the particular systems.²⁷ This is since more and more phonon modes become populated with T increasing. Compared with the BC_3 sheet, interestingly, there appear several crossings in C_V curves of the various BCNTs at different T . These crossings are attributed to the first optical phonon modes excited at different T_{op} in different BCNTs. In the cases of CNTs, the predicted ω_{op} and T_{op} have been observed in specific heat experiments, showing a unique quantized phonon structure.²⁸ Our work indicates that the quantized phonon structures may be universal in quasi-1D nanotube systems, which may be observed in the BCNTs. At room temperature, also, we calculate in the Fig. 4(b) the specific heat of the armchair (n,n) and zigzag $(n,0)$ BCNTs as a function of n . From Fig. 4(b), C_V of both (n,n) and $(n,0)$ BCNTs increase with the tube diameter increasing, and reach the value of the BC_3 sheet. This feature is due to the fact that DOS of larger tube-diameter BCNTs is close to the BC_3 sheet, in which the PDR of BCNTs can be given by the zone-folding from the PDR of the BC_3 sheet. For a given n , obviously, C_V of a (n,n) BCNT is larger than that of a $(n,0)$ BCNT, the same as in the case of CNTs.¹² The same trends in the (n,n) and $(n,0)$ CNTs can be seen in Fig. 4(b) inset. These interesting behaviors may also be universal for quasi-1D nanotube systems. To understand the physical origin of this universal behavior, we now calculate the PDR of CNTs within a zone folding method. In spite of the defi-

ciency in low frequency region, the intermediate and high frequency phonon modes can be described well by this model.²⁹ Here we take the armchair (n,n) CNTs as an example. The 1D PDR of CNTs is given by^{8,29}

$$\omega_{1D}^{m\mu}(k) = \omega_{2D}^m \left(k \frac{K_2}{|K_2|} + \mu K_1 \right), \quad (6)$$

with $m=1,2,\dots,6$, $\mu=0,1,\dots,N/2-1$, and $-\pi/T < k \leq \pi/T$, where N is the number of atoms in the unit cell, K_1 and K_2 the unit wave vectors in the circumferential and axial directions, $\omega_{2D}^m(k)$ the 2D PDR of a graphite sheet, k the 1D continuous wave vector, and T is the magnitude of translation vector in the axis. The discrete value of μ is the consequence of wave vector quantization in the circumferential direction. Figure 5(a) shows the 2D Brillouin zones of $(5,5)$ and $(10,10)$ CNTs. Due to the similar symmetry of $(5,5)$ CNT with $(10,10)$ CNT, the wave vectors of $(5,5)$ CNT just correspond to one-half of those of $(10,10)$ CNT. Therefore,

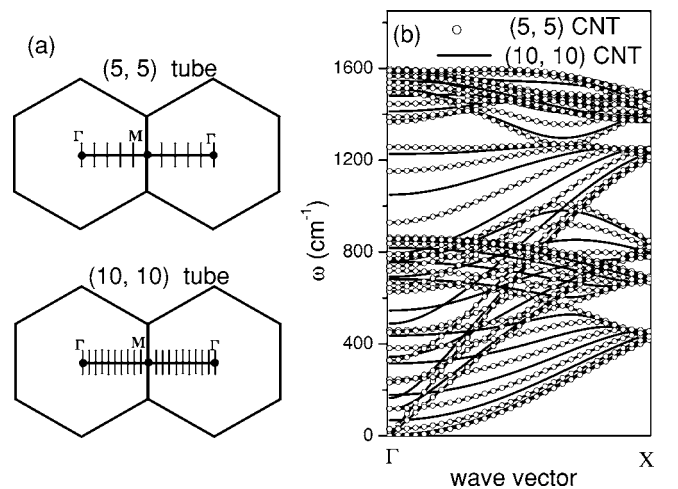


FIG. 5. (a) The 2D Brillouin zones of $(5,5)$ and $(10,10)$ CNTs; (b) PDR of armchair $(5,5)$ CNT (open circles), and $(10,10)$ CNT (solid lines).

the PDR of (5,5) CNT is completely included in that of (10,10) CNT, as shown in Fig. 5(b). Similar relation between (n,n) and (nl,nl) tubes can be derived, where l is an integer other than 1. In terms of this relation, the specific heat of a (n,n) tube can be directly related to that of a (nl,nl) tube. Changing the integral into the summation, Eq. (5) is rewritten as

$$C_V(T) = k_B \sum_{q,j} \left(\frac{\hbar \omega_j(q)}{k_B T} \right)^2 \frac{e^{\hbar \omega_j(q)/k_B T}}{(e^{\hbar \omega_j(q)/k_B T} - 1)^2}, \quad (7)$$

with $j=1,2,\dots,3N$, where q is the wave vector and $\omega_j(q)$ is the frequency of q phonon mode. Since $\omega_j(q)$ of (5,5) tube is only the part of that of (10,10) tube, C_V of (5,5) tube is smaller than that of (10,10), i.e., $C_V^{(5,5)} < C_V^{(10,10)}$. Similarly, one can obtain $C_V^{(n,n)} < C_V^{(nl,nl)}$. In the limit of $n \rightarrow \infty$, on the other hand, the discrete wave vectors of a (n,n) tube would turn into a continual 2D Brillouin zone. In this case, PDR of the CNT is consistent with that of 2D graphite sheet, and thus C_V of the CNT approaches the limit of 2D graphite C_V^{2D} . As a result, an alternative formula of $C_V^{(n,m)}$ can be obtained by

$$C_V^{(n,m)} = C_V^{2D} - E/R^\alpha, \quad (8)$$

with E the scaling factor and α the scaling exponent. Eq. (8) directly links the specific heat of a nanotube to that of a 2D sheet, and shows the intrinsic relationship between thermal properties of the nanotube and its geometrical structures. Actually, the derivation of Eq. (8) is regardless of its compositions of the nanotube, which is in good agreement with the fitted formulas of C_V in CNTs.⁷ Therefore, Eq. (8) may show a universal behavior of C_V in various types of quasi-1D nanotube systems.

IV. CONCLUSIONS

In summary, we investigate the phonon dispersion relation and specific heat of the BC₃ sheet and BCNT within a force constant model. The force constant parameters have been obtained by fitting the phonon spectrum of BC₃ sheet to the experimental data. The phonon spectra of BCNTs are calculated in terms of these force constants, of which the number of distinct phonon branches is four times larger than that of CNTs. It is shown that the frequencies of RBM and the lowest phonon mode E_{2g} of BCNTs are dependent on the tube diameter, fitted well by the power law relations with various scaling parameters, which is at variance with CNTs and BN nanotubes. These scalings may be very helpful in the future to characterize BCNTs for fast selection in nanotube samples. Moreover, the specific heat of BCNTs is calculated, less than that of the BC₃ sheet. Due to the difference of the first optical phonon mode, several crossings in specific heat of various BCNTs have been observed, which may suggest the underlying quantized phonon structures in BCNTs. A universal relation between the specific heat of a nanotube and its geometrical structure is derived, which can provide a useful help to explore quantum size effects and universal laws in quasi-1D nanotube systems.

ACKNOWLEDGMENTS

This work is supported by the National Natural Science Foundation of China under Grant Nos. 10374046 and 10447129, the Hunan Provincial Natural Science Foundation of China under Grant No. 04JJ3041, the Program for New Century Excellent Talents in University under Grant No. NCET-04-0779, and partially by the Hunan Provincial Research Foundation of Education Bureau of China under Grant No. 03B039 and the Undergraduate Innovation Fund of Xiangtan University.

*Email address: jwding@xtu.edu.cn

¹Z. Weng-Sieh, K. Cherrey, N. G. Chopra, X. Blase, Y. Miyamoto, A. Rubio, M. L. Cohen, S. G. Louie, A. Zettl, and R. Gronsky, Phys. Rev. B **51**, R11229 (1995).

²Y. Miyamoto, A. Rubio, S. G. Louie, and M. L. Cohen, Phys. Rev. B **50**, 18360 (1994).

³Y. H. Kim, K. J. Chang, and S. G. Louie, Phys. Rev. B **63**, 205408 (2001).

⁴E. Hernandez, C. Goze, P. Bernier, and A. Rubio, Phys. Rev. Lett. **80**, 4502 (1998).

⁵S. Reich, C. Thomsen, and J. Maultzsch, *Carbon Nanotubes: basic concepts and physical properties* (Wiley-VCH, Cambridge, 2004).

⁶Y. Xiao, X. H. Yan, J. X. Cao, J. W. Ding, Y. L. Mao, and J. Xiang, Phys. Rev. B **69**, 205415 (2004).

⁷J. X. Cao, X. H. Yan, Y. Xiao, Y. Tang, and J. W. Ding, Phys. Rev. B **67**, 045413 (2003).

⁸J. Nagamatsu, N. Nakagawa, T. Muranaka, Y. Zenitani, and J. Akimitsu, Nature (London) **410**, 63 (2001).

⁹R. Saito, G. Dresselhaus, and M. S. Dresselhaus, *Physical Prop-*

erties of Carbon Nanotubes (Imperial College Press, London, 1998).

¹⁰R. Saito, T. Takeya, T. Kimura, G. Dresselhaus, and M. S. Dresselhaus, Phys. Rev. B **57**, 4145 (1998).

¹¹V. N. Popov, V. E. Van Doren, and M. Balkanski, Phys. Rev. B **59**, 8355 (1999).

¹²E. Dobardzic, I. Milosevic, B. Nikolic, T. Vukovic, and M. Damjanovic, Phys. Rev. B **68**, 045408 (2003).

¹³S. M. Bachilo, M. S. Strano, C. Kittrell, R. H. Hauge, R. E. Smalley, and R. B. Weisman, Science **298**, 2361 (2002).

¹⁴A. Jorio, R. Saito, J. H. Hafner, C. M. Lieber, M. Hunter, T. McClure, G. Dresselhaus, and M. S. Dresselhaus, Phys. Rev. Lett. **86**, 1118 (2001).

¹⁵R. Pfeiffer, H. Kuzmany, Ch. Kramberger, Ch. Schaman, T. Pichler, H. Kataura, Y. Achiba, J. Kurti, and V. Zolyomi, Phys. Rev. Lett. **90**, 225501 (2003).

¹⁶S. Bandow, S. Asaka, Y. Saito, A. M. Rao, L. Grigorian, E. Richter, and P. C. Eklund, Phys. Rev. Lett. **80**, 3779 (1998).

¹⁷H. Telg, J. Maultzsch, S. Reich, F. Hennrich, and C. Thomsen, Phys. Rev. Lett. **93**, 177401 (2004).

- ¹⁸D. Sanchez-Portal and E. Hernandez, *Phys. Rev. B* **66**, 235415 (2002).
- ¹⁹E. Rokuta, Y. Hasegawa, K. Suzuki, Y. Gamou, C. Oshima, and A. Nagashima, *Phys. Rev. Lett.* **79**, 4609 (1997).
- ²⁰L. Wirtz, A. Rubio, R. A. de la Concha, and A. Loiseau, *Phys. Rev. B* **68**, 045425 (2003).
- ²¹H. Yanagisawa, T. Tanaka, Y. Ishida, M. Matsue, E. Rokuta, S. Otani, and C. Oshima, *Phys. Rev. Lett.* **93**, 177003 (2004).
- ²²O. E. Alon, *Phys. Rev. B* **63**, 201403 (R) (2001).
- ²³M. Damnjanovic, T. Vukovic, I. Milosevic, and B. Nikolic, *Acta Crystallogr., Sect. A: Cryst. Phys., Diffr., Theor. Gen. Crystallogr.* **57**, 304 (2001).
- ²⁴T. Yamamoto, S. Watanabe, and K. Watanabe, *Phys. Rev. Lett.* **92**, 075502 (2004).
- ²⁵J. Kurti, G. Kresse, and H. Kuzmany, *Phys. Rev. B* **58**, R8869 (1998).
- ²⁶Y. Xiao, Z. M. Li, X. H. Yan, Y. Zhang, Y. L. Mao, and Y. R. Yang, *Phys. Rev. B* **71**, 233405 (2005).
- ²⁷V. N. Popov, *Phys. Rev. B* **66**, 153408 (2002).
- ²⁸J. Hone, B. Batlogg, Z. Benes, A. T. Johnson, and J. E. Fischer, *Science* **289**, 1730 (2000).
- ²⁹R. A. Jishi, L. Venkataraman, M. S. Dresselhaus, and G. Dresselhaus, *Chem. Phys. Lett.* **209**, 77 (1993).